

Evaluation of the structural cap for the integrated flood wall system of New Orleans

Sudarshan Adhikari¹ Student M. ASCE, Chung R. Song² M. ASCE, Alexander H.D. Cheng³ F. ASCE, and Ahmed Al-Ostaz⁴ M. ASCE

This study is specifically motivated to evaluate the effectiveness of the structural cap by using the three dimensional finite difference code equipped with elasto-plastic material models for the soil and soil/structure interface. To evaluate the effectiveness of the structural cap, three cases are dealt which are likely to lead the localized failure of I-wall in New Orleans:(1) The spatial variability of the soil strength in the New Orleans region with weak zones localized in some spots along the I-wall promoting a local levee breaches in that portion. (2) Localized erosion of some weak erodible soil portion of I-wall section. (3) Localized structural failure of the individual panel of I-wall which might be due to the weak bondage between the sheet pile and the concrete capping.

¹ Graduate Assistant, Department of Civil Engineering, University of Mississippi, Carrier 121L, University, MS 38677; E-mail: sadhikar@olemiss.edu

² Associate Professor, Department of Civil Engineering, University of Mississippi, Carrier 218, University, MS 38677; E-mail: csong@olemiss.edu

³ Professor and Dean , Office of Dean, School of Engineering, University of Mississippi, Carrier 101, University, MS 38677; E-mail: acheng@olemiss.edu

⁴ Associate Professor, Department of Civil Engineering, University of Mississippi, Carrier 204, University, MS 38677; E-mail: alostaz@olemiss.edu

From the study, it was found that the structural cap is effective in restricting the relative displacement of the adjacent panels but is not that effective in reducing the overall displacement of the system significantly in first two cases listed above but it is very effective to reduce the overall displacement of the system in the third case. The other interesting result from the study is that the spatial variation of the strength along the flood wall and the non uniform erosion results the higher bending moment about the vertical axis which is not addressed by the current design guidelines.

Introduction

During the Hurricane Katrina, the major causes of the breaches were due to the instability of I-wall sections. There are many reasons that led to the failure of I-walls. One of those reasons that led to the failure of this type of flood wall is that the flood wall didn't behave as if it is one integral system. This non integrity of the system might arise from the improper or weak bondage between the concrete capping and the sheet pile depth wise or the composition of I-wall as different panels of varying length (USACE 2001) length wise acting individually without behaving in mutually supportive manner so that the intolerable stresses developed in one of the individual panel has to be bear individually without getting any chance of sharing stresses with the adjacent section thus leading to the localized failure.

Three cases are dealt in this study which causes the localized failure of I-wall in New Orleans. The spatial variation of the soil strength in the New Orleans region having weak spots is one of the main causes for the local levee breaches in that region. For example in 17th street Canal, according to USACE (2006), the measured shear strength of levee fill material varies widely

from 120 psf to 5000 psf. Similar is the case for peat where the measured shear strengths vary from about 50 to 920 psf. So the strength parameters used in the design may not represent fully the actual strength of the soil of that region. This can be understood by illustration in Fig. 1.

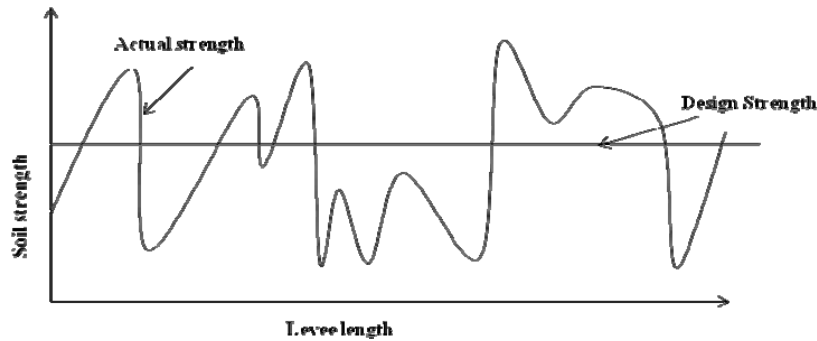


Fig1: Conceptual graph showing the difference of actual and design strength

From Fig.1, it can be inferred that the I-wall sections having actual strength above the design strength will have the factor of safety more than what is required in the design guidelines but the sections where the strength falls below the design strength will have the factor of safety below the required one. So from the figure, it can be concluded that the region where the actual strength falls below the design strength will have higher probability of failure as compared to the regions where the actual strength is above the design strength. This indicates that only some sections of I-wall are vulnerable to instability. But in terms of the catastrophe induced by this local failure, no matter how small it is, it is not insignificant. And at the same time reducing the design strength to the lower bound of the actual strength distribution or improving the soil to bring up the actual strength up to design strength may be too uneconomic. So it is necessary to find an alternative mechanism which is economic and at the same time effective to get rid of this problem.



Fig2: Local Failure of one panel (IPET V-14-64)

The other cause of the local failure is related to the erosion of some weak erodible soil portion of I-wall section. During hurricane Katrina, it was observed that some parts of I-wall section were suffered from erosion. This led the separation of two adjacent concrete panels resulting uncontrolled erosion induced by entrance of the flood water through the gap of separation promoting the expansion of the scour leading catastrophe.

Last but not least, the local failure of the I-wall might be caused by the local structural failure of the individual panel due to the the weak bondage between the sheet pile and the concrete capping. Though there is no evidence of such failure during hurricane Katrina, this case is felt to be investigated since it has the potential to be occurred in future, since the I-wall system in New Orleans is very old that the interface between the concrete capping and the sheet pile is so weak promoting the propensity of plastic hinge at the junction between the two.

The main objective of this study is to integrate the isolated panel into one system so that the whole I-wall will act as if it is one unit. This integral unit will take the advantage of the stress redistribution in the unit so that the weak section enjoys the sharing of the stresses with the strong section relieving the overstressed zone and thus preventing it from the progression of failure.

One of the mechanisms of integrating the flood wall system that the project has proposed is the use of the structural cap. The structural cap is simply a structural element combining two adjacent panels at the top of the wall devised to restrict the relative displacement between them and aid in distribution of the stresses from the overstressed panel to the under-stressed panel. The schematic of the location of the cap and the individual panel is shown in Fig.3.

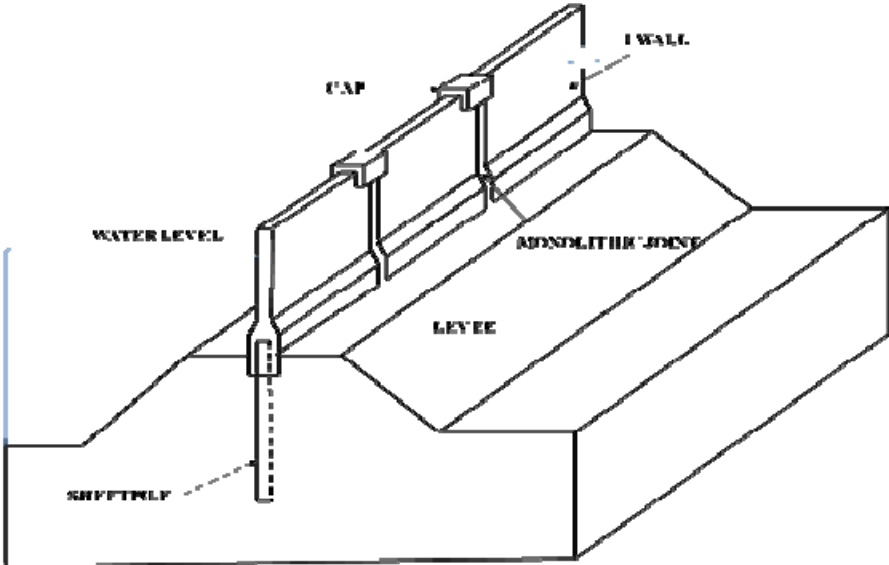


Fig 3: Schematics of I- wall showing individual panels with structural cap

Numerical Simulation

FLAC^{3D} Geometric Model

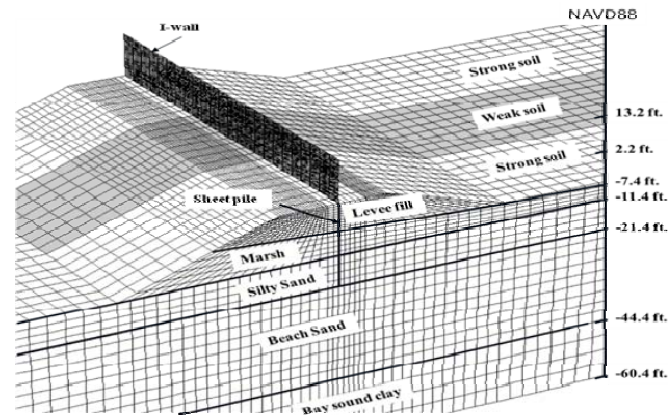


Fig 4: FLAC^{3D} Geometric Model

For numerical modeling, one of the critical sections of London Avenue Canal is taken. The geological set up of the site consists of four natural soil layers such as bay sound clay, beach sand, silty sand and the marsh. The embankment of lean or fat clay overlay the marsh layer up to 2.2 feet in NAVD88 Scale. Above the embankment is I-wall which propels up to 13.2 feet. Sheet pile is embedded in to the soil up to -21.4 feet. The depth of each of these layers represented in NAVD88 scale is shown in Fig. 4. The characteristics of the FLAC3D numerical model are:

1. Soil is represented by the brick type zones each having eight grid points possessing elasto- plastic behavior.
2. Sheet pile and the concrete capping are represented by linearly elastic two dimensional shell type finite elements known as the 'embedded liner' slaved with an interface.
3. As the boundary condition, all the movement at the bottom level of the computational were restricted whereas at the lateral exterior sides, the lateral movement was restricted

To simplify the building up of FLAC^{3D} model, sheet pile is assumed to be installed up to crest level which is joined to the concrete capping above it. The use of shell element for the concrete capping against solid zones is to capture the bending effects accurately and to reduce the computational time. The sheet pile is created to be one unit but as far as the concrete capping is considered, it is separated into three separate units which idealize three different panels of realistic I-wall. The geometrical simplification used in the modeling is shown in Fig. 5:

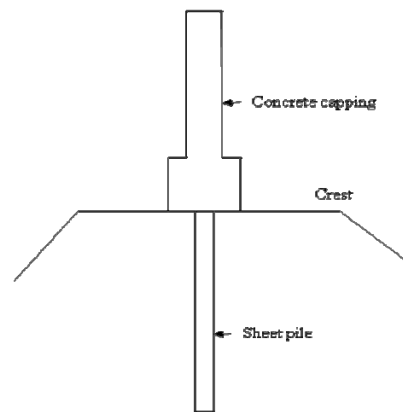


Fig 5: Model simplification at the sheet pile and the concrete capping joints

Figure needs correction to reflect the embedded section.

To model cap, the ideal case is adopted in which the top 2 feet of the adjacent panels are rigidly connected which is possible by using the link elements of FLAC^{3D} possessing rigid degree of freedoms in all directions. In this study we are only trying to investigate the performance of cap in ideal case, the details of the cap structure and its interaction with the concrete panel is beyond the scope of this study and should be investigated separately.

To account for the soil strength variation of first case of this study, the model is idealized to be divided in to three sections in out of plane direction of equal lengths (the length of the panel of I-wall, in this study: 24 feet) in which the section with weak soil is sand-witched between the

sections with strong soil as shown in Fig.4. But in two other cases, the soil in longitudinal direction is taken to be homogenous of intermediate strength.

Soil parameters and soil constitutive model

The soil parameters derived in our previous study was used for the second and third cases. For the first case, main concern of the study is the effect of the soil strength variation in the longitudinal direction to the overall behavior of the flood wall system and the remedy action required to reduce the problem created by this situation. It is seen that in one of the region (17th Street Canal) near the study site, there is a wide variability of the shear strength of the soil for marsh and levee fill materials but the variation is not of much significance for the sand layer and stiff clay underneath (IPET 2007). So in the 3D numerical analysis, the variation of the soil strength is related to the embankment soil and the marsh soil only. Two extreme strengths were taken where the lower bound of the strength represents the strength for weak soil and the upper bound represents the strength for the strong soil. In Fig. 5, two extreme bounds of soil strengths are categorized as weak and strong soil strength.

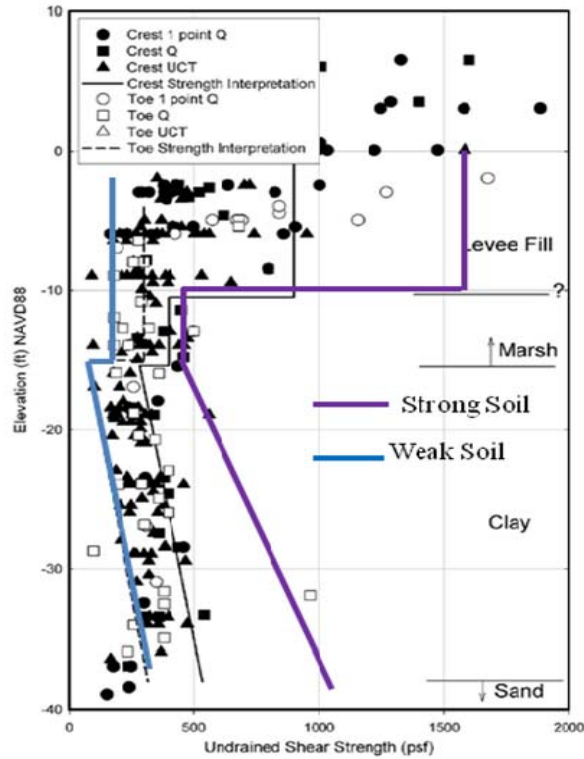


Fig 6: Scattered undrained shear strength for cohesive soil in 17th Street Canal with upper and lower bound strengths (Data obtained IPET, 2009)

Stiffness parameters are calculated using the undrained elastic modulus using some calibrated factors from our previous study. As far as the Poisson's ratio is considered, it is assumed to be 0.48 for the cohesive soil; 0.41 for beach sand and 0.43 for silty sand respectively. The details of soil strength parameters are discussed in our previous paper. The soil parameters are shown in the Table 1.

Tresca elasto- perfectly plastic soil model was used for the cohesive soil and Mohr coulomb plastic model was used for cohesion less soil.

Table1: Soil parameters

Soil layer	Shear Strength			Saturated density (Slug/cf)	Elastic modulus (Psf)			Poisson's ratio
	weak	Intermediate	strong		weak	Intermediate	strong	
Levee-fill	Su=200 Psf, $\phi_u=0^\circ$	Su=900 Psf, $\phi_u=0^\circ$	Su=1600 Psf, $\phi_u=0^\circ$	3.39	1.84E+04	8.28E+04	1.47E+05	0.48
Marsh(Toe)	Su=200 Psf, $\phi_u=0^\circ$	Su=300 Psf, $\phi_u=0^\circ$	Su=450 Psf, $\phi_u=0^\circ$	2.49	5.52E+04	8.28E+04	1.24E+05	0.48
Marsh(Center)	Su=200 Psf, $\phi_u=0^\circ$	Su=400 Psf, $\phi_u=0^\circ$	Su=450 Psf, $\phi_u=0^\circ$	2.49	5.52E+04	1.10E+05	1.24E+05	0.48
Bay sound Clay		Su=5000 Psf, $\phi_u=0^\circ$		3.89		5.52E+06		0.48
Relic Beach Sand		$c'=0$, $\phi'=36^\circ$		3.79		4.83E+05		0.41
Silty Sand		$c'=0$, $\phi'=31^\circ$		3.66		2.76E+05		0.43

Model parameters for the soil–wall interface:

Structural element of the FLAC^{3D}, known as ‘embedded liner’ has been used to model the sheet pile. Apart from having structural behavior of the shell type element, the embedded liner also has the tangential and normal interaction between it and the FLAC^{3D} grid. This tangential and the normal behavior is controlled by the embedded liner interfacial properties. This means that the embedded liner has the interface slaved with it so that building of separate interface is not necessary.

The normal behavior of the soil- sheet pile interface is governed by the normal coupling springs properties like the stiffness per unit area, K_n and the tensile strength f_t . The tangential or the shear behavior of the soil sheet pile interface is governed by the shear coupling springs properties like stiffness per unit area, K_s ; cohesive strength c ; residual cohesive strength c_r ; the friction angle ϕ and the interface normal stress σ_n . The tangential behavior of the interface is so modeled that if the interface fails in tension, then the effective cohesion drops from c to residual cohesion c_r and the tensile strength is reduced to zero. But if the relative displacement is such that there is no more separation between the soil and the sheet pile, then the normal stress will again develop. This behavior of the liner interface in FLAC^{3D} provides the possibility of modeling gap occurrence and closing of it very accurately. Fig.7 and Fig. 8 show the normal and shear directional behavior of the interface.

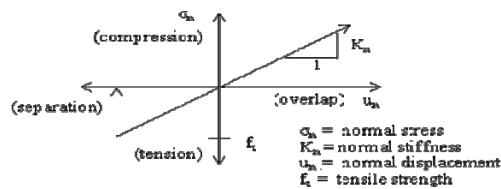
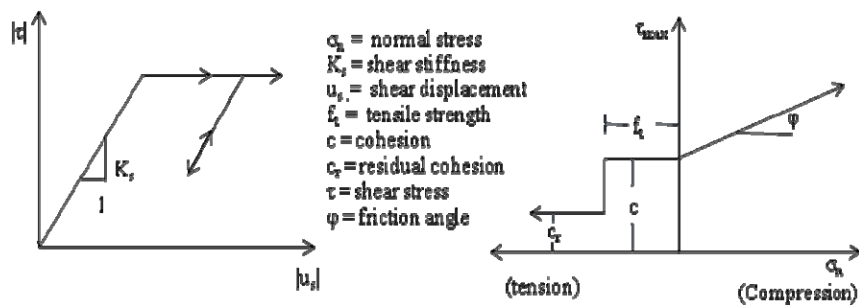


Fig.7: Normal directional interface behavior for sheet pile (Adapted from Itasca, 2006)



(a) Shear stress versus total relative displacement

(b) shear-strength criterion

Fig. 8: Shear-directional interface behavior for sheet pile (Adapted from Itasca, 2006)

Schematic of the FLAC^{3D} interface elements showing constitutive behavior are shown in Fig.9.

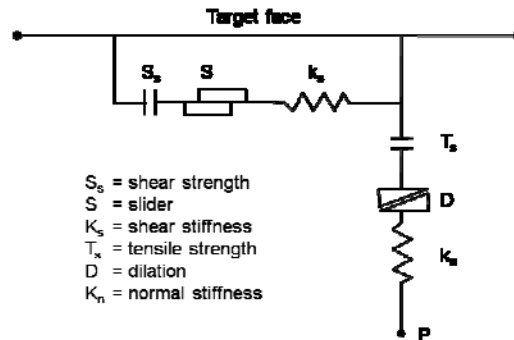


Fig. 9: Components of soil/wall interface constitutive model (Adapted from Itasca, 2006)

As mentioned earlier, the main interfacial properties required for the simulation are the stiffness and the strength parameters. The FLAC^{3D} manual (Itasca 2006) points out that the strength properties of the interface are important, but the stiffness properties are not. But if there is a large contrast of the stiffness in the system, it takes a lot of time for numerical simulation to converge. So to economize the simulations, the FLAC^{3D} Theory and Background Manual (Itasca 2006) recommend that the K_n and K_s can be estimated by rule of thumb which is to be 10 times the stiffest neighboring zone.

$$K_n \approx K_s \approx 10. \max \left[\frac{K + \frac{4}{3}G}{\Delta z_{\min}} \right] \quad (1)$$

Where K & G are the bulk and shear Moduli respectively and Δz_{\min} is the smallest width of an adjoining zone in the normal direction. The max [] notation indicates that the maximum value over all the zones adjacent to the interface to be used.

As far as the strength parameters of the interface are concerned, for cohesive soil, they are given in terms of cohesion which is equal to 0.5 to 0.7 times the undrained strength of the adjacent soil (Bowles 1996). In this Simulation, the cohesion is estimated using the relation:

$$c \approx 0.67.S_u \quad (2)$$

Where, S_u denotes the undrained shear strength of the adjacent soil and c is the cohesion of interface.

For the case of cohesion less soil, the strength parameters are given in terms of angle of friction. For steel pile embedded in silty sand (dirty sand), the interface angle of friction, δ is taken to be 14° (Bowles 1996; USACE 1994).

Model parameters for I-wall

Capping

To model concrete capping and sheet pile, structural element of the FLAC^{3D}, known as “embedded liner” was used. The structural element is basically the shell element having resistance to both membrane loading and the bending loading. The shell element in FLAC^{3D} can possess either of the isotropic, orthotropic or anisotropic properties. In this simulation, initially, I-wall is assumed to possess an isotropic elastic property (if the moment is beyond the limiting tensile strength, then the cracking was considered resulting anisotropic property). It requires three parameters to define the mechanical properties of these elements: density, ρ ; elastic modulus, E ; Poisson’s ratio, ν ; and the thickness, t . The density of the concrete is readily available in any literature. The Poisson’s ratio of concrete ν can vary from 0.15 to 0.2 (give the

reference if any). In this simulation the Poisson's ratio is assumed to be 0.2. The young's modulus of normal weight concrete is estimated using the relation (Wang et al. 1998):

$$E_c = 57,000 \cdot \sqrt{f'_c} \quad (3)$$

Where, E_c is the elastic modulus of Concrete in psi and f'_c is the compressive strength of the concrete that varies from 3500 to 5000 psi for usual non pre-stressed reinforced concrete (Wang et al. 1998). In this numerical simulation it is taken to be 3925 psi. This value is an average value of the compressive strength measured by taking samples from the existing I-wall. The details can be found in Appendix 15, Volume V of IPET report (IPET 2007)

For the reinforced concrete structures, the moment of inertia for uncracked section can be estimated using the relation:

$$I_{uncr} = \frac{1}{12}bD^3 + (n-1)A_s h_s^2 + (2n-1)A'_s h_s'^2 \quad (4)$$

In the analysis, the flexural stiffness corresponding to the moment of inertia calculated by equation (4) can be used provided that the bending moment induced by the analysis is less than the cracking moment M_{cr} . If the bending moment is more than the cracking moment, then the flexural stiffness corresponding to moment of inertia for the partially or fully cracked section should be used.

The moment of inertia for cracked section can be estimated using the relation (Everad 1993):

$$I_{cr} = \frac{b(kd)^3}{3} + (2n-1)A'_s (kd - d')^2 + nA_s (d - kd)^2 \quad (5)$$

Where n is the modular ratio given by the relation:

$$n = \frac{E_s}{E_c} \quad (6)$$

Taking E_s to be 29,000,000 psi and E_c to be 3,571,040 psi n comes to be 8.12 and

$$k = \sqrt{[n\rho + (2n-1)\rho']^2 + 2[n\rho + (2n-1)\rho' d' / d]} - [n\rho + (2n-1)\rho'] \quad (7)$$

$$\rho = \frac{A_s}{bd} \quad (8a)$$

$$\rho' = \frac{A'_s}{bd} \quad (8b)$$

In modeling, to account the composition of reinforcement in the section either we can use the actual thickness of the wall section with equivalent modulus moment of inertia corresponding to cracked or uncracked section; or the modulus of concrete with equivalent thickness interpreted from the moment of inertia for the cracked or uncracked section.

The equivalent modulus of elasticity can be calculated adopting that the rigidity for two aforementioned conditions are same i.e.

$$I_{uncr(cr)} E_c = I_c E_e \quad (9)$$

Evaluating,

$$E_e = \frac{I_{uncr(cr)} E_c}{I_c} \quad (10)$$

Where I_c corresponds to the real section of the wall.

And the equivalent thickness of the shell element can be estimated using the following relation

$$t_e = \sqrt[3]{\frac{12 * I_{uncr(cr)}}{b}} \quad (11)$$

To see the effect of crack and the reinforcement on the deflection and the bending stress development in I-wall, sensitivity analysis was conducted for stiffness corresponding to plain concrete section, uncracked reinforced concrete section and the cracked reinforced concrete section .The result is shown and discussed as below:

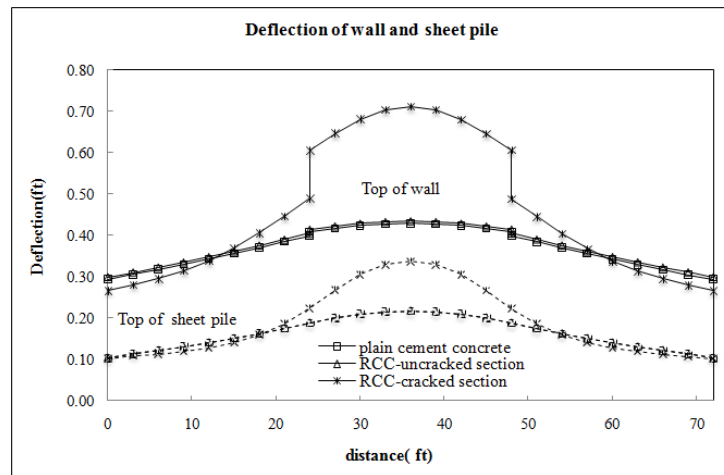


Fig 10: Deflection of the wall and the sheet pile

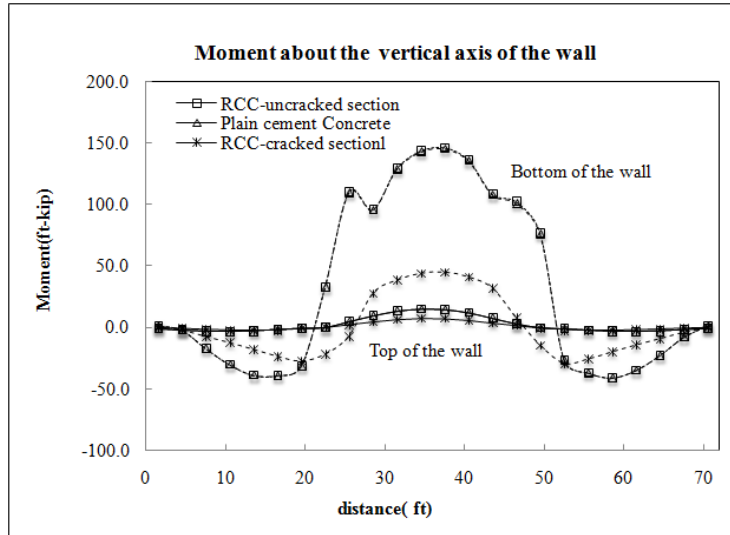


Fig 11: Moment about the vertical axis of the wall

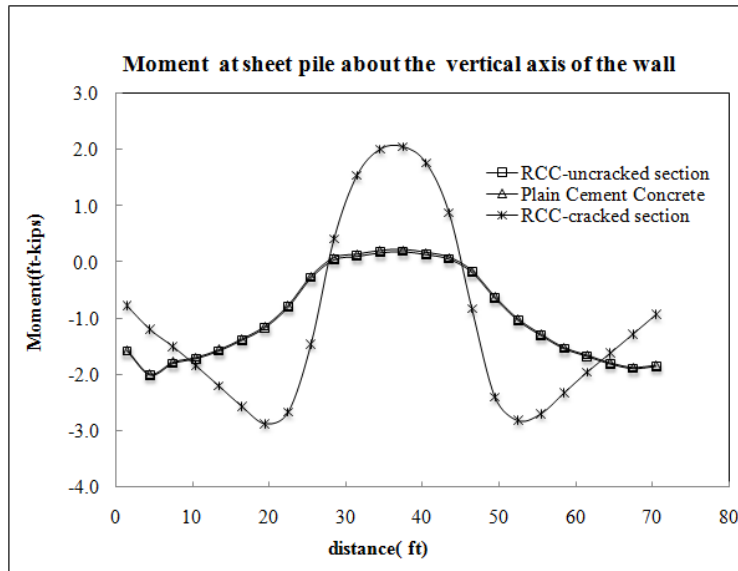


Fig 12: Moment at the sheet pile about the vertical axis of the wall

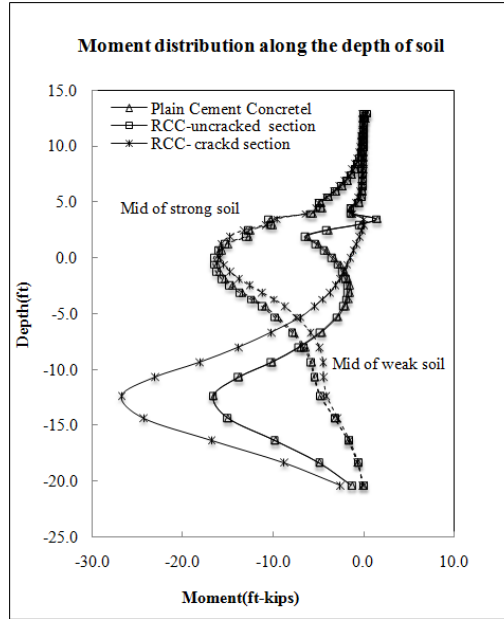


Fig 13: Moment about horizontal axis of the wall

From the result it can be seen that as far as the crack is not considered in the concrete section, the deflection and the moment distribution is not different for the composite reinforced concrete and the plain cement concrete. But if we use the cracked section to calculate the stiffness of I-wall section, then the difference is very large. From this result, it might be wrong to avoid the cracking of the concrete in the analysis.

The main concern in this study is that which modulus should be taken during the numerical analysis. Normally when the deflection (serviceability) is the main concern, the cracked moment of inertia should be taken into account (Everad 1993). But still it is customary to use uncracked section and see if the concrete on the tensile side is within the tensile strength given by the equation (12a) (ACI 318-05, 2005) or not

$$f_{ct} = 7.5\sqrt{f'_c} \quad (12a)$$

Or,

$$M_{cr} = \frac{2 \cdot f_{ct} \cdot I_{uncr}}{D} \quad (12b)$$

Only in case when the tensile stress is beyond that given in equation (12), the reduced stiffness may be used.

Actually, for reinforced concrete, however, three different flexural stiffness values can be considered: the uncracked stiffness; transition from uncracked to cracked stiffness; and the cracked stiffness. This can be illustrated using a moment curvature diagram for a length of beam shown in the Fig. 14. Fig. 15 shows the distribution of EI along the beam where the stiffness varies from the uncracked value at points where the moment is less than the cracking moment to a partially cracked value at points of higher moment. Therefore in the transition from the uncracked condition to the fully cracked condition, the reinforced concrete section may have the different flexural stiffness depending upon the curvature or the moment induced in the structure.

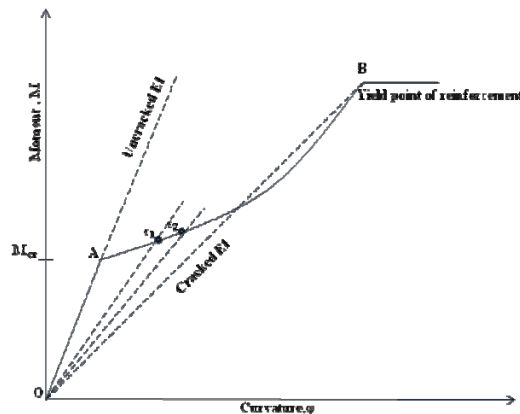


Fig. 14: Moment–curvature curve for the reinforced cement concrete section (Adapted from MacGregor 1992)

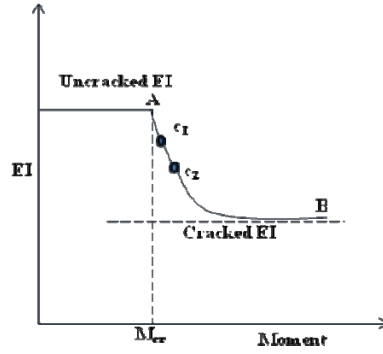


Fig. 15: Variation of the Stiffness of the reinforced cement concrete with moment ((Adapted from MacGregor 1992))

Actually, modeling the crack propagation is beyond the scope of this study and is not incorporated in this study. But still it is possible to incorporate the variation of the flexural stiffness due to the variation of the curvature or moment induced in the system. Though the yielding of the reinforced cement concrete cannot be modeled for the FLAC structural element (linear elastic model), but still using this procedure, we will be able to judge accurately whether the loading condition has already reached the moment capacity or not.

The other method to capture the cracking of the RCC section is to calculate the effective moment of inertia which can be calculated as the following equation (Branson 1971). This method will be more appropriate in hand calculation since the distribution of the EI is very hard to be incorporated in such case.

$$I_e = \left(\frac{M_{cr}}{M_a} \right)^a I_{uncr} + \left[1 - \left(\frac{M_{cr}}{M_a} \right)^a \right] I_{cr} \quad (13)$$

Where, M_a is the maximum moment in the member at the loading stage for which the moment of inertia is being computed or any previous loading stage.

But as long as we are using numerical simulation, it is more appropriate to use the stiffness calculated using the first criterion discussed above. So in this analysis, we may conduct the analysis using the uncracked section and check whether the tensile and the compressive strength are within the compressive and the tensile strength of the concrete or not. If tensile stress crosses the limiting stress provided in equation (12a), we need to repeat the analysis using the cracked moment of inertia.

The equation for this condition is given by:

$$EI = (EI)_{uncracked} \quad \text{if } M < M_{cr} \quad (14)$$

$$EI = \frac{M}{M_{cr} / (EI)_{uncracked} + \frac{(M - M_{cr}) * (\phi M_n / (EI)_{cracked} - M_{cr} / (EI)_{uncracked})}{(\phi M_n - M_{cr})}} \quad \text{if } M > M_{cr} \quad (15)$$

$$EI = (EI)_{cracked} \quad \text{if } M > \phi M_n \quad (16)$$

Now using the equations above, the variation for the stiffness for the real I-wall sections (**New Design Guidelines**) are calculated and the variations is shown in the Fig. 16.

From Fig. 16 it is seen that the I-wall section recommended in the new design guidelines is seen to be quite brittle. Since the ductility is provided mostly by the steel reinforcement, it can be inferred that the I-wall sections are provided with very less reinforcement which exhibits brittleness.

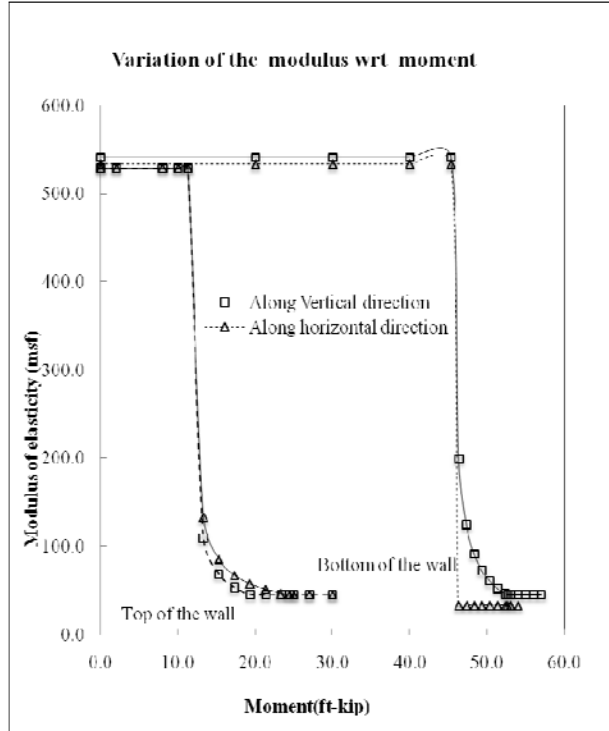


Fig. 16: Variation of the Stiffness of the reinforced cement concrete with moment for I-wall section

Sheet pile

The sheet pile used in London Avenue canal is CZ-101(USACE 2008). The geometrical parameters of this type of sheet pile are found in the manufacturer table (sheetpile.net). To account the simple geometry of the shell element used in the simulation against the complex one of the real Z-type sheet pile, equivalent thickness of the shell element is estimated using the relation:

$$t_{eq} = \sqrt[3]{I} \tag{13}$$

Where, t_{eq} denotes the equivalent thickness of the embedded liner element used in the simulation

and I denotes moment of inertia in in^4 per unit foot width of the sheet pile

A variation of soil strength in the longitudinal direction in a 3 dimensional analysis has a prominent effect of anisotropy of bending stiffness on the bending moment and the deflection of wall. Since the degree of anisotropy is an uncertain parameter and to see to what extent of anisotropy has its significant effect on the bending and deflection of I-wall, sensitivity analysis was conducted. The results were compared for five cases: the isotropic case; and the orthotropic case with 10, 100, 1000 and 1000 times reduced rigidity in horizontal direction.

The stiffness matrix for the isotropic plate can be calculated by the following relation (FLAC^{3D} 2006):

$$\begin{aligned}
 c_{11} = c_{22} &= \frac{E}{1-\nu^2} \\
 c_{33} &= \frac{E}{2(1+\nu)} \\
 c_{12} &= \nu \left(\frac{E}{1-\nu^2} \right) \\
 c_{13} = c_{23} &= 0
 \end{aligned} \tag{14}$$

For the orthotropic material, the constitutive equation can be represented as:

$$\{ \sigma' \} = \begin{Bmatrix} \sigma_{x'} \\ \sigma_{y'} \\ \tau_{x'y'} \end{Bmatrix} = [E'] \{ \epsilon' \} = \begin{bmatrix} c'_{11} & c'_{12} & 0 \\ sym. & c'_{22} & 0 \\ & & c'_{33} \end{bmatrix} \begin{Bmatrix} \epsilon_{x'} \\ \epsilon_{y'} \\ \gamma_{x'y'} \end{Bmatrix} \text{ (orthotropic shell)} \tag{15}$$

The stiffness matrix for orthotropic material can be divided into membrane stiffness and the bending stiffness, which can be calculated as (Ugural 1981):

$$\begin{aligned}
 c'_{11} &= \frac{E'_{x'}}{1-\nu_{x'}\nu_{y'}} \\
 c'_{22} &= \frac{E'_{y'}}{1-\nu_{x'}\nu_{y'}} \\
 c'_{33} &= G
 \end{aligned} \tag{16}$$

$$c'_{12} = \frac{E'_x \nu'_{y'}}{1 - \nu'_x \nu'_{y'}} = \frac{E'_y \nu'_{x'}}{1 - \nu'_x \nu'_{y'}}$$

Where $E'_x, E'_y, \nu'_x, \nu'_{y'}$ are the modulus and poisons ratio along the local axes x' and y' respectively.

$$\begin{aligned} c^{b'}_{11} &= \frac{12}{t^3} D_{x'} \\ c^{b'}_{22} &= \frac{12}{t^3} D_{y'} \\ c^{b'}_{33} &= \frac{12}{t^3} G_{x'y'} \\ c^{b'}_{12} &= \frac{12}{t^3} D_{x'y'} \end{aligned} \tag{17}$$

Where $D_{x'}, D_{y'}, D_{x'y'}$ and $G_{x'y'}$ represent the flexural rigidities and the torsional rigidities respectively. If $D_{x'}$ and $D_{y'}$ are known then $D_{x'y'}$ and $G_{x'y'}$ can be calculated using the relation: (Ugural 1981)

$$\begin{aligned} G_{x'y'} &= \frac{1 - \nu}{2} \sqrt{D_{x'} D_{y'}} \\ D_{x'y'} &= \nu \sqrt{D_{x'} D_{y'}} \end{aligned} \tag{18}$$

Graphs for the deflection at top and the center of the wall; deflection at the bottom and the center of the wall; moment M_x at top and bottom of the wall; moment at the top of the sheet pile; and moment M_y at center of the sheet pile are compared.

The result from the study is shown in the figure below:

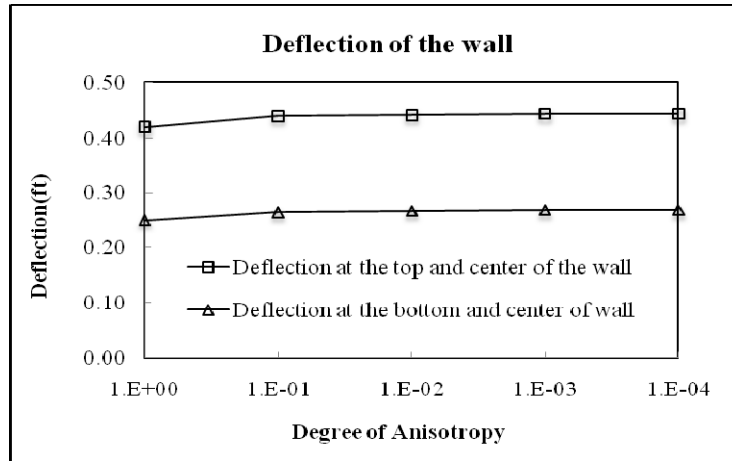


Fig 10: Deflection of the wall for different degree of anisotropy

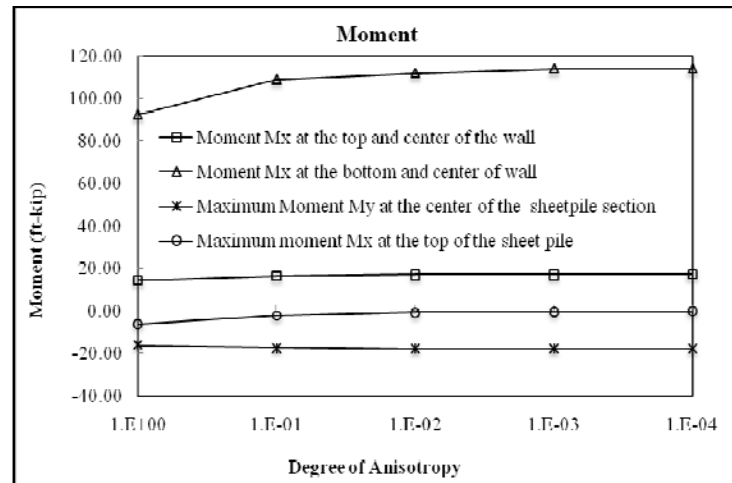


Fig 11: Moment at the wall and Sheet pile for different degree of anisotropy

From Fig. 10 and Fig. 11, it can be seen that as the anisotropy increases, the deflection and the moment M_x (moment about vertical axis) of the wall increases but the moment on sheet pile section decreases. From the figures, it can also be seen that the anisotropy is much influential when the degree of anisotropy (the ratio of horizontal modulus of elasticity to the vertical modulus of elasticity) is 0.1. The increase in anisotropy beyond this magnitude is seen to be not that influential. So in this study, we assumed that the degree of anisotropy is 0.1.

Cases of study

There are many potential causes for the localized failure of I-wall. Out of those potential failure modes, three cases are investigated in this study: variation of soil strength along I-wall section; localized erosion of certain part of the soil section along the I-wall; weak bondage between the sheet pile and the concrete capping due to the result of the rusting of the sheet piles or due to the poor workmanship during the casting of the sheet pile rendering the concrete capping and the sheet pile to act as the separate entities at certain location of the I-wall section. Each of these cases is investigated in this study to find out for which case the cap would be more effective.

Case 1: Variation of Soil Strength

One of the failure mechanisms of the failure of I-wall in New Orleans during Katrina was due to soil instability at weak soil spots. During hurricane Katrina, instead of the collapse of the whole system only some portion was breached. The example of such breach was that of the 17th street Canal Breach which was of the length 450 feet (Duncan 2008). These wide breaches were not developed in one shot but were developed by the sequence of inception and progression of the local and small scale breaches which occurred due to the localized weaker zones. So if only the onset of these small scale breaches is inhibited by some mechanism, the development of the larger breaches might be out of question. So effectiveness of the cap as the mechanism to restrict the onset of this localized failure is investigated in this study.

In the analysis, to model the extreme case, the development of the gap up to sand layer and the reduction of strength of the marsh stratum at higher water level are incorporated in the soil section having weak strength.

Two steps were conducted during the analysis as mentioned earlier. In the first step the cracking was not include in the analysis and to see if the stresses are within the tensile strength of the concrete or not. Then if the stresses cross the limit then the cracking was incorporated using the relation given by the equations (14-16).

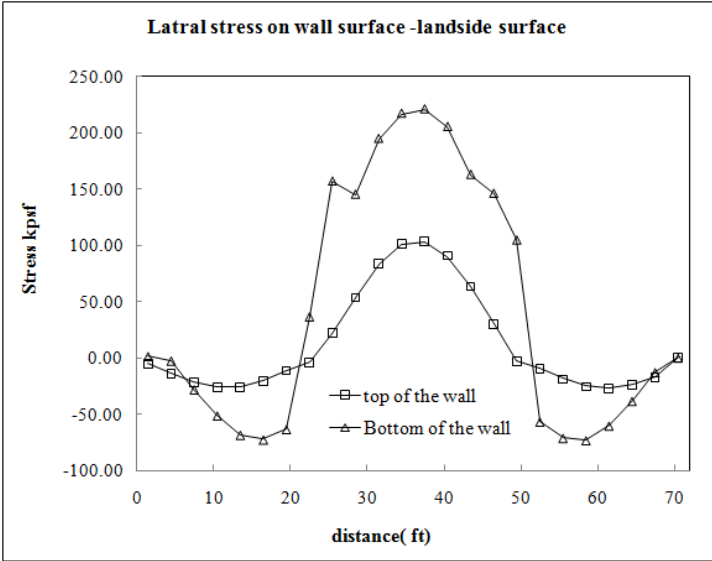


Fig. 12: Lateral stress on the wall surface

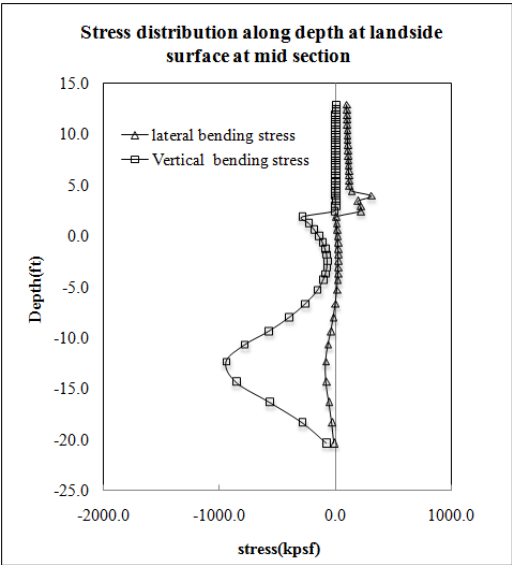


Fig. 13: Stress distribution along the depth at surface at mid section

From Fig.12, it is seen that the bending stress has already reached the tensile strength of the concrete given by Eq. (12a) which is 67.7 Ksf. So it was necessary to use the stiffness derived by incorporating cracking.

To see the effect of cap, deflection at top of the wall; deflection at the bottom of the wall; deflection along the center of the wall; moment at the top of the wall; moment at the bottom of the wall; and moment at the center of the wall are compared for the I-wall with and without cap. These are illustrated in the figures below.

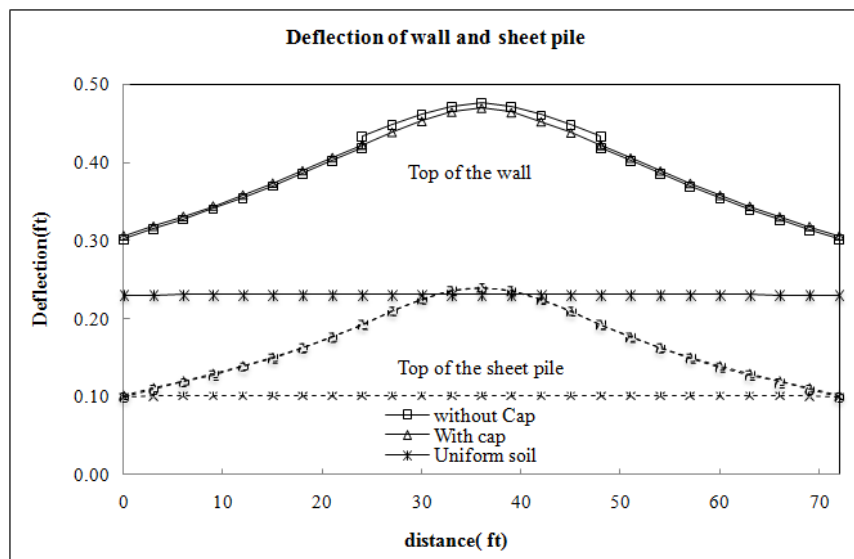


Fig 14: Deflection of the wall and the sheet pile

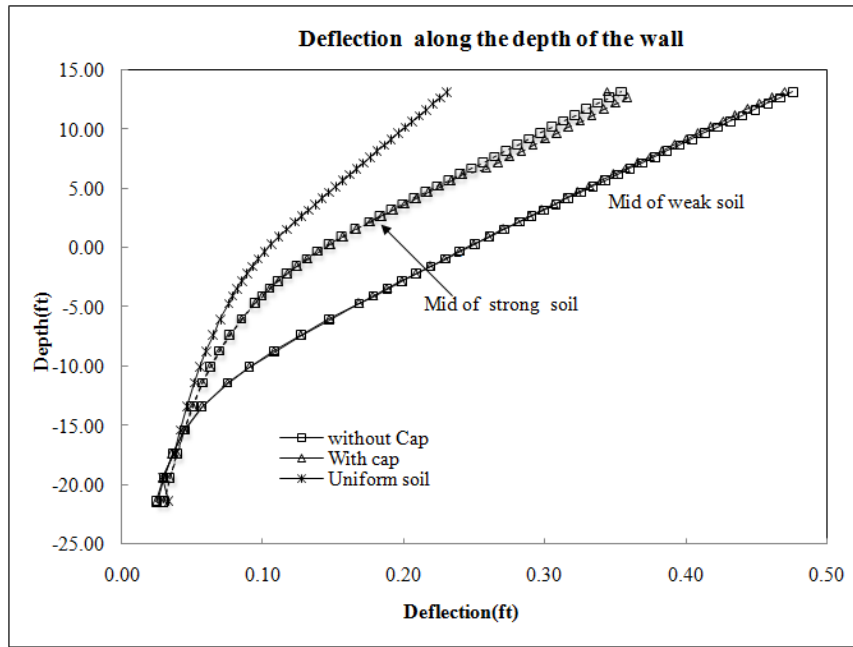


Fig 15: Deflection of the wall and the sheet pile along depth

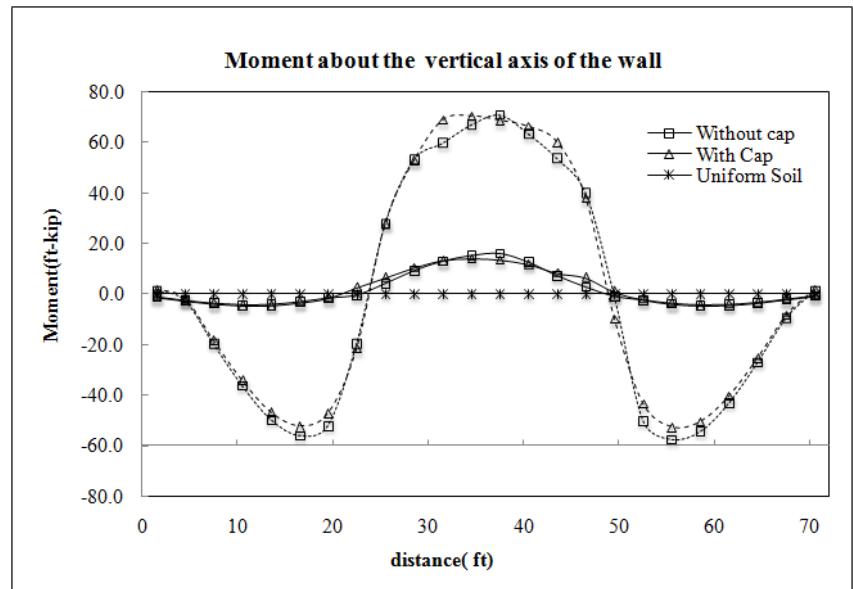


Fig 16: Moment about the vertical axis of the wall

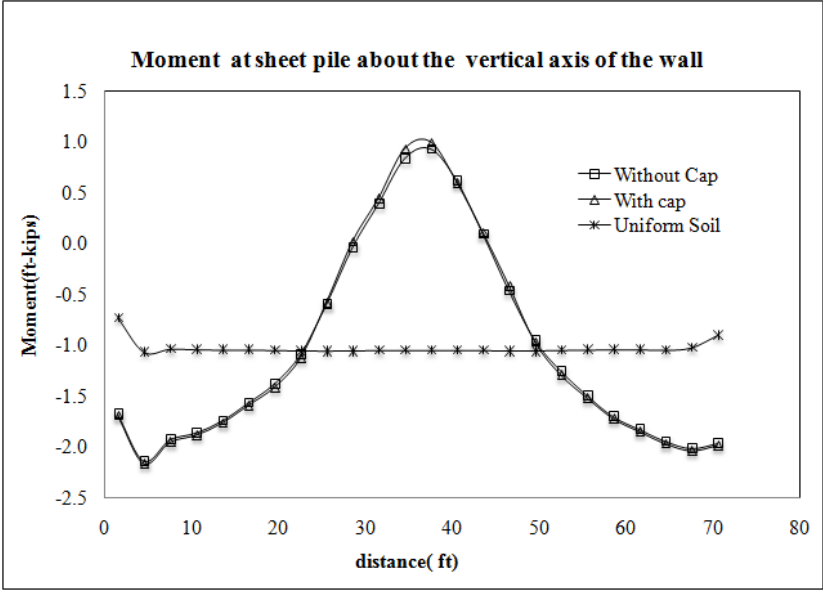


Fig 17: Moment at the sheet pile about the vertical axis of the wall

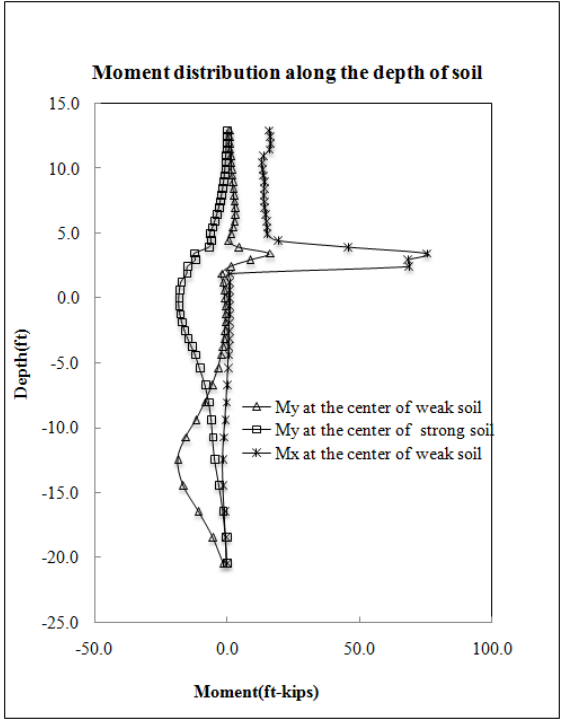


Fig 18: Moment about vertical axis of the wall (M_x) and about horizontal axis of the wall (M_y)

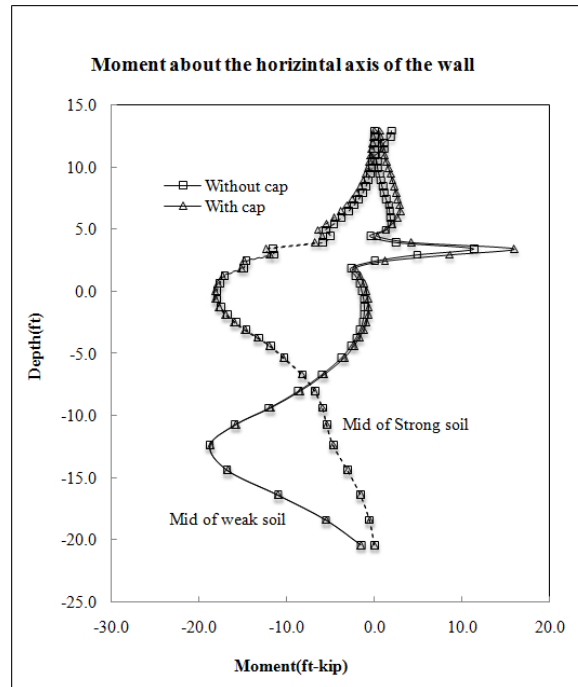


Fig 19: Moment about horizontal axis of the wall

Discussion of the result

From Fig. 14, it can be seen that the relative displacement for two adjacent panels at the top of the wall is reduced when the cap is used. But at the same time the incorporation of the cap is not that effective in reducing the overall displacement of I-wall. There is also not much significant improvement of the moment distribution in the wall when the cap is used. With this result, we can still stick to the point that since the relative displacement of two adjacent panels is not allowed; the impending failure of the weak panel is resisted to some extent by the strong panel inhibiting the local failure of the weaker panel.

From the result it can also be seen that the moment induced by the variation of the soil strength about the vertical direction is much greater than the moment about the lateral direction due to the hydrostatic loading. This provokes us to think whether the I-wall section related to the current

design guidelines is strong enough to resist the moment attributed to the spatial variation of the soil strength or not. To investigate this, we compare the moment of resistance of the available section of the typical I-wall of New Orleans with the computed bending moment. Fig.20 shows the typical cross section of I-wall used for the analysis.

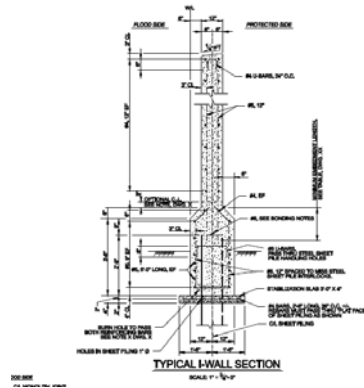


Fig 20: Typical cross section of I wall (adapted from USACE 2008)

The cross sections at the top of the wall and the bottom of the wall above the ground level is shown in Fig. 18

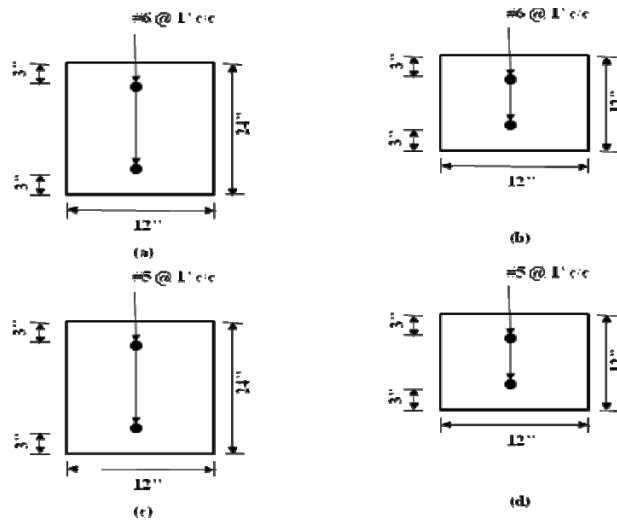


Fig. 21: Typical cross section of the wall

- (a): Lengthwise per unit foot at the bottom of the wall
- (b): Lengthwise per unit foot at the top of the wall
- (c): Depth wise per unit foot at the bottom of the wall
- (d): Depth wise per unit foot at the top of the wall

The design check is done for the **true strength** available from the testing of samples collected and **design strength** recommended in ASTM code

From the IPET report, Volume 5, Appendix 15 (real value from the sampling), the compressive strength of the concrete, f'_c is 3925 psi and yield strength of the steel bar, f_y is 71 ksi. And for the design value recommended by ASTM A 615, f'_c is 3 ksi and f_y is 60 ksi

Two assumptions are adopted to calculate the moment of the resistance of the wall and the minimum is taken to be the one which is compared with the bending moment computed from FLAC^{3D}. But since the compression still and the tension steel are of equal in area for the typical section, **assumption 2** would be valid since the compressive reinforcement would not subjected to the yield stress. The Moment of resistance calculated is using the following equations (MacGregor 1992)

Assumption 1: Compressive reinforcement subjected to yield stress

$$M_n = \phi \left[(A_s - A'_s) f_y (d - a/2) + A'_s f_y (d - d') \right] \quad (20)$$

Assumption 2: Compressive reinforcement not subjected to yield stress

$$M_n = \phi \left[C_c \left(d - \frac{a}{2} \right) + C_s (d - d') \right] \quad (21)$$

Where,

$$C_c = 0.85 f'_c b a \quad (22)$$

and

$$C_s = (E_s \varepsilon'_s) A'_s = E_s A'_s \left(1 - \frac{\beta_1 d'}{a} \right) 0.003 \quad (23)$$

Where a is given by the relation,

$$(0.85 f'_c b) a^2 + (0.003 E_s A'_s - A_s f_y) a - 0.003 E_s A'_s \beta_1 d' = 0 \quad (24)$$

In the above equations, β_1 is taken to be 0.85

Using above relations, the moment of resistance for the four sections listed above is calculated and compared with the computed bending moment. The comparison is shown in the table 2.

Table2: Comparison of bending moment with the moment of resistance

S/N	Section	Moment of resistance (ft-lb)				Computed moment (ft-lb)
		real strength		ASTM design strength		
		Assumpt.1	Assumpt.2	Assumpt.1	Assumpt.2	
1	a	40,416.75	52,629.62	34,155.00	44,045.38	18200
2	b	12,593.63	24,430.92	10,642.50	20,222.76	5990
3	c	28,681.78	39,175.00	24,238.13	32,825.03	70500
4	d	8,872.78	19,366.00	7,498.13	16,085.03	13390

Similarly we also investigated if the sheet pile is yielded or not. As far as the moment in the sheet pile is considered, the tensile stress in the sheet pile can be calculated as:

$$\sigma_t = M / z \quad (25)$$

Where z is the section modulus and is given by:

$$z = \frac{bt^2}{6} \quad (26)$$

Where t is the thickness of the sheet pile. The section modulus per unit foot of the sheet pile of this study is 0.2178 ft^3

For this case, maximum moment in the sheet pile computed by FLAC^{3D} is 18800 lb-ft (M_y) and 2140 lb-ft (M_x). For these moments, the stresses developed in the sheet pile using equation (25) due to M_y is 0.60 ksi and due to M_x is 0.068 ksi which are far below the yield strength of the sheet pile. The yield strength of the sheet pile measured by getting the sample was 56.6 ksi whereas the value recommended using the [ASTM A 328](#) is 39 ksi. From this comparison, it is seen that the sheet pile will still be safe on account of soil strength variation.

Case 2: Erosion

In this case erosion is so idealized that it is considered to be taken place on the soil section corresponding to central panel whereas the other parts are not affected by the erosion. During hurricane Katrina, the largest depth of the scour was found to be 6.5 feet ([Seed et al. 2008](#)) and the longest breach that took place during Katrina was of 920 feet ([Seed et al. 2008](#)). Seed et al. (2008) points out that this length of breach probably has been occurred in a progressive manner which starts from the small section scouring. This small section scouring might have brought the non uniform deflection of the I-wall resulting misalignment of the I-wall which then opened the gap between the individual panels making a way for the water to flow through this gap resulting an uncontrolled erosion thus expanding the scouring along the length leading to the wider breach. So the main point is if some mechanism is there to restrict the misalignment of the I-wall section, then this might restrict the uncontrolled erosion which ultimately reduces the width of

the scouring and thus preventing it from having a wide breach. This is investigated in this study and we had the following results.

Two steps were conducted during the analysis as mentioned earlier. In the first step the cracking was not include in the analysis and to see if the stresses are within the tensile strength of the concrete or not. Then if the stresses cross the limit then the cracking was incorporated using the relation given by the equations (14-16).

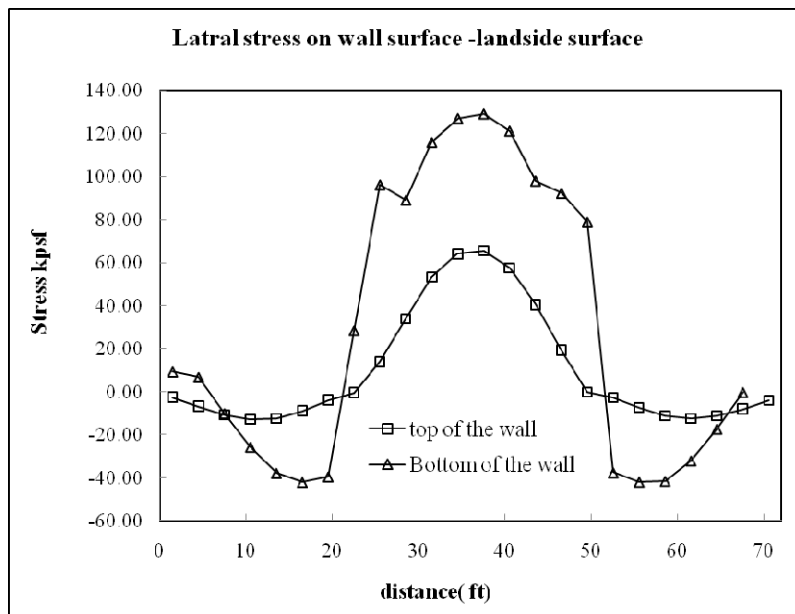


Fig. 21: Lateral stress on the wall surface

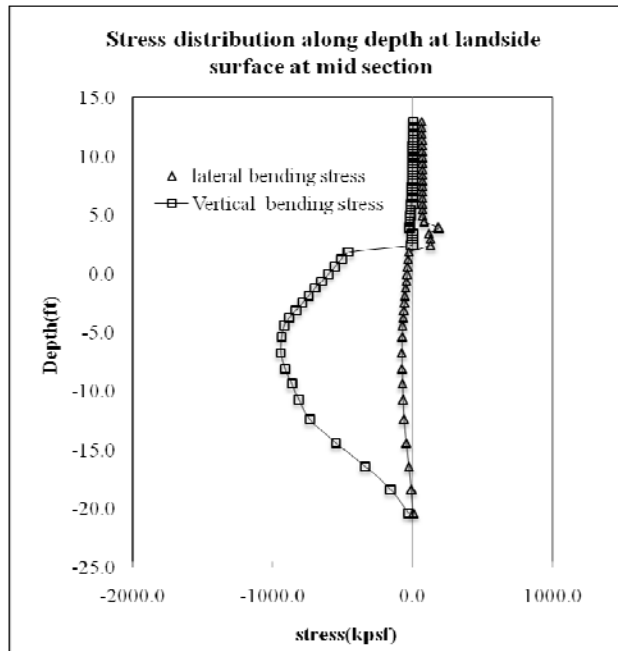


Fig. 22: Stress distribution along the depth at surface at mid section

From Fig. 21, it is seen that the bending stress has already reached the tensile strength of the concrete given by Eq. (12a) which is 67.7 Ksf. So it was necessary to use the stiffness derived from using cracking. So we repeated the analysis using cracking.

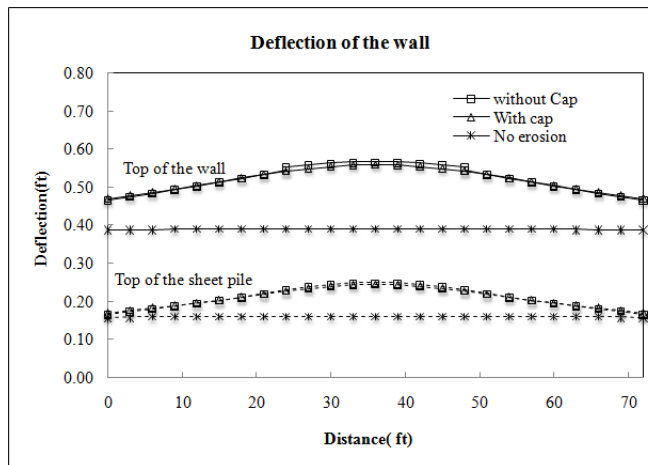


Fig 23: Deflection of the wall and the sheet pile

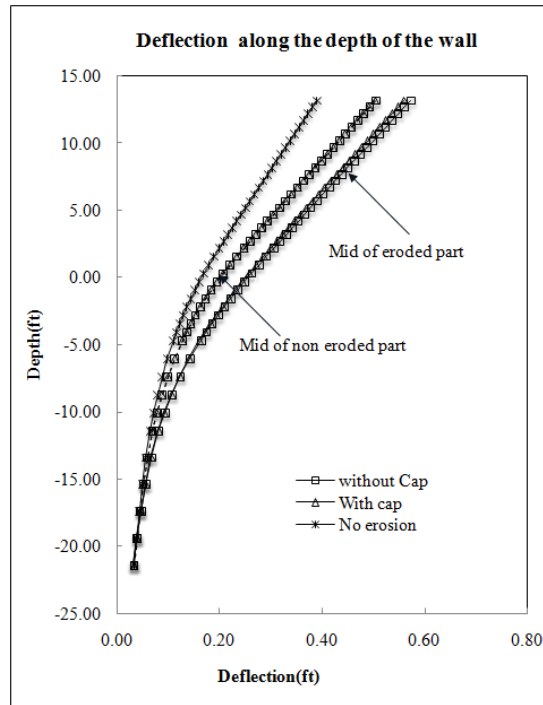


Fig 24: Deflection of the wall and the sheet pile along depth

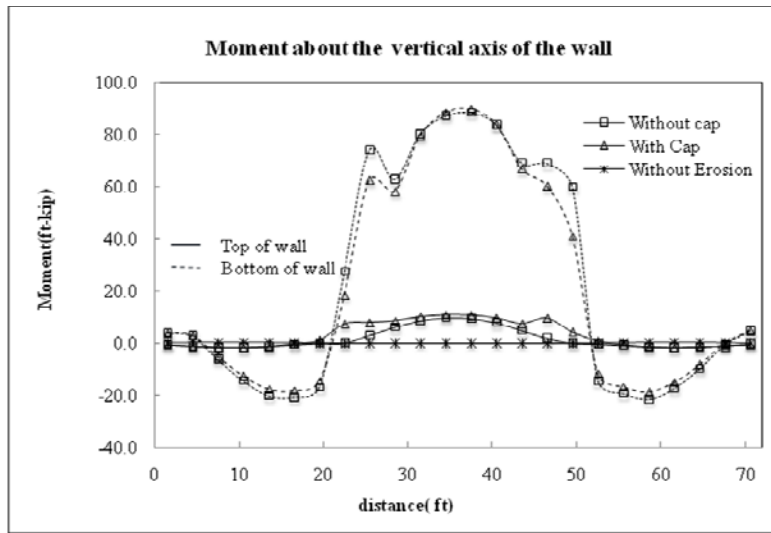


Fig 25: Moment about the vertical axis of the wall

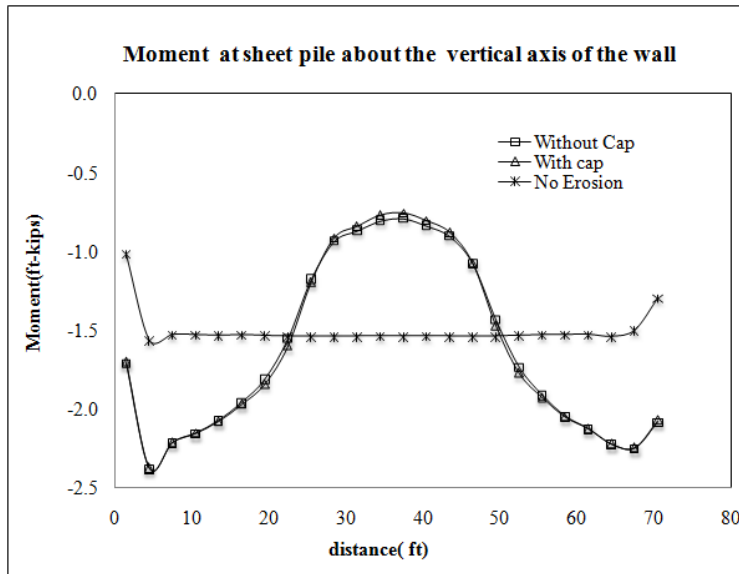


Fig 26: Moment at the sheet pile about the vertical axis of the wall

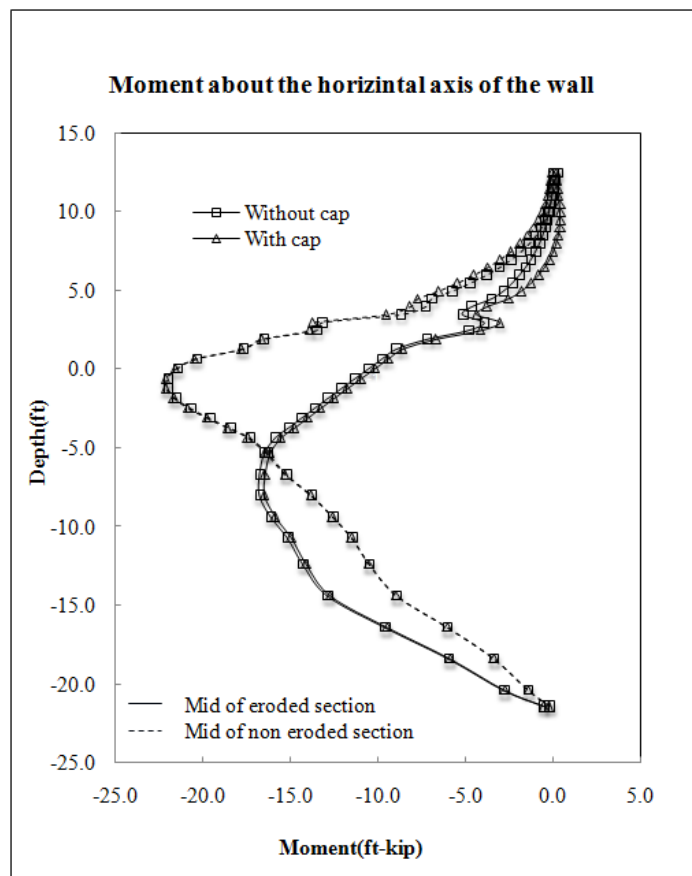


Fig 27: Moment about horizontal axis of the wall

As in the first case, there has been a reduction of the relative displacement on the two adjacent panels when cap is installed but the overall deflection and the distribution of the moment has not been improved. As in the first case, the computed moment and the moment of the resistance of the typical I-wall is compared and is shown in the Table 3:

Table 3: Comparison between the computed bending moment and the moment of resistance

S/N	Section	Moment of resistance (ft-lb)				Computed moment (ft-lb)
		Real strength		ASTM Design Strength		
		Assumpt.1	Assumpt.2	Assumpt.1	Assumpt.2	
1	a	40,416.75	52,629.62	34,155.00	44,045.38	16500
2	b	12,593.63	24,430.92	10,642.50	20,222.76	8150
3	c	28,681.78	39,175.00	24,238.13	32,825.03	90200
4	d	8,872.78	19,366.00	7,498.13	16,085.03	11000

In this case also, maximum moment in the sheet pile computed by FLAC^{3D} is 16700 lb-ft(M_y) and 2380 lb-ft(M_x). For these moments, the stresses developed in the sheet pile due to M_y is 0.53 ksi and due to M_x is 0.074 ksi which are far below the yield strength of the sheet pile. So the sheet pile is not yielded for this case.

Case 3: Plastic hinge

In this case, the weak bondage between the sheet pile and the concrete capping is considered. Here, the weak bondage is simulated using the plastic hinge at the joint between the sheet pile and the concrete capping. This type of failure mechanism was not observed during Katrina but it is felt to be important since this might be the potential failure for the old levee system like New

Orleans which is attributed to the deterioration of the material through the rusting. The results are shown in the figures below.

Two steps were conducted during the analysis as mentioned earlier. In the first step the cracking was not include in the analysis and to see if the stresses are within the tensile strength of the concrete or not. Then if the stresses cross the limit then the cracking was incorporated using the relation given by the equations (14-16).

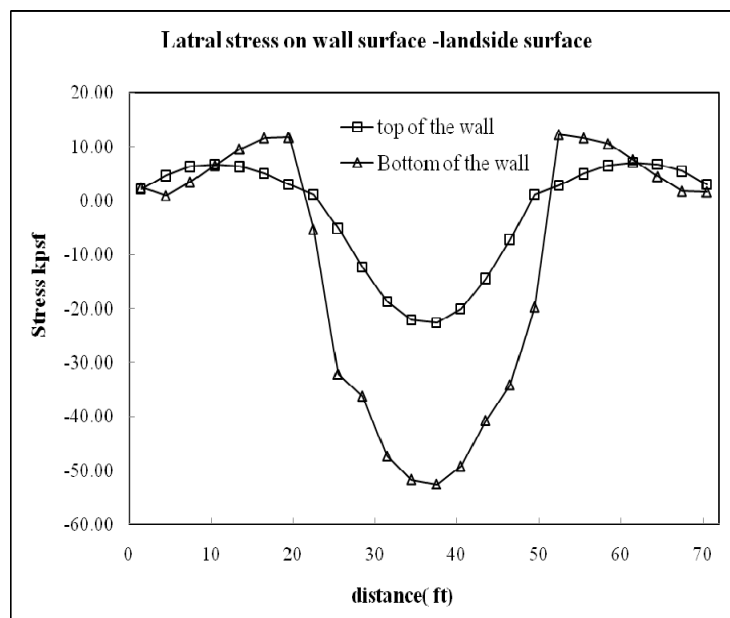


Fig. 28: Lateral stress on the wall surface

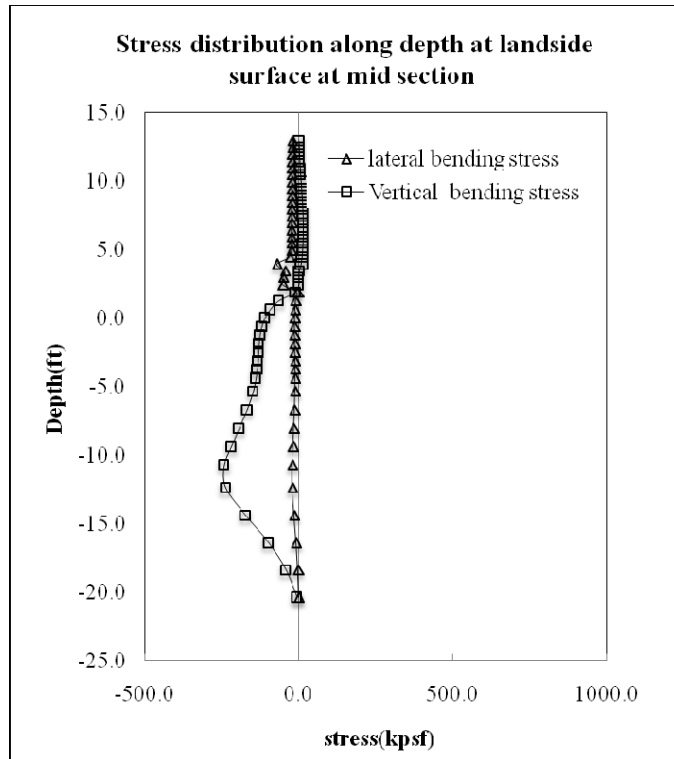


Fig. 29: Stress distribution along the depth at surface at mid section

From Fig. 28 and 29, it is seen that the bending stress is below the tensile strength of the concrete given by Eq. (12a) which is 67.7 Ksf. So it was not necessary to use the stiffness derived from cracking. The stiffness of the uncracked section can be used for the analysis in this case.

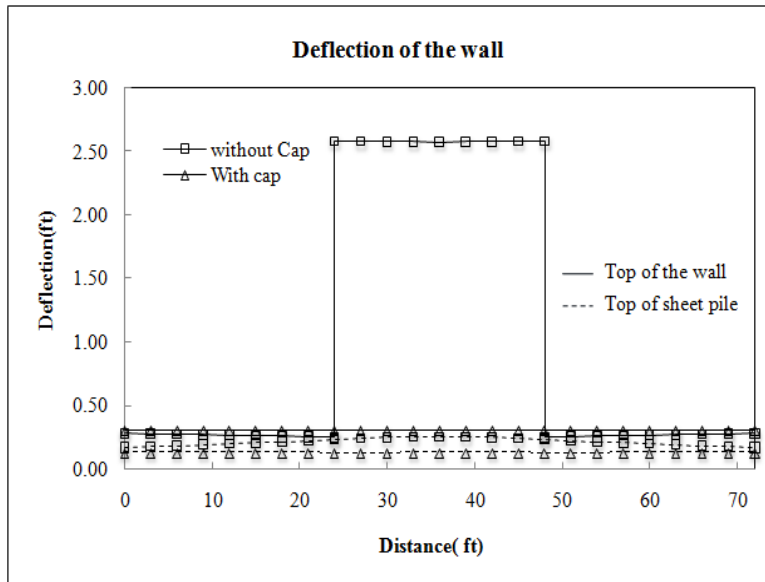


Fig 30: Deflection of the wall and the sheet pile

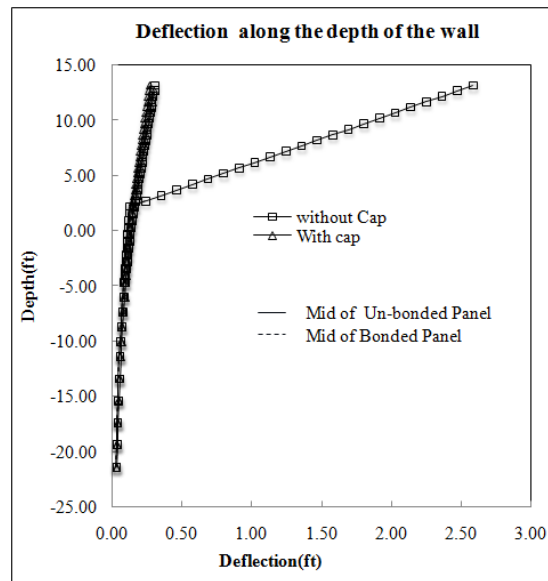


Fig 31: Deflection of the wall and the sheet pile along the depth

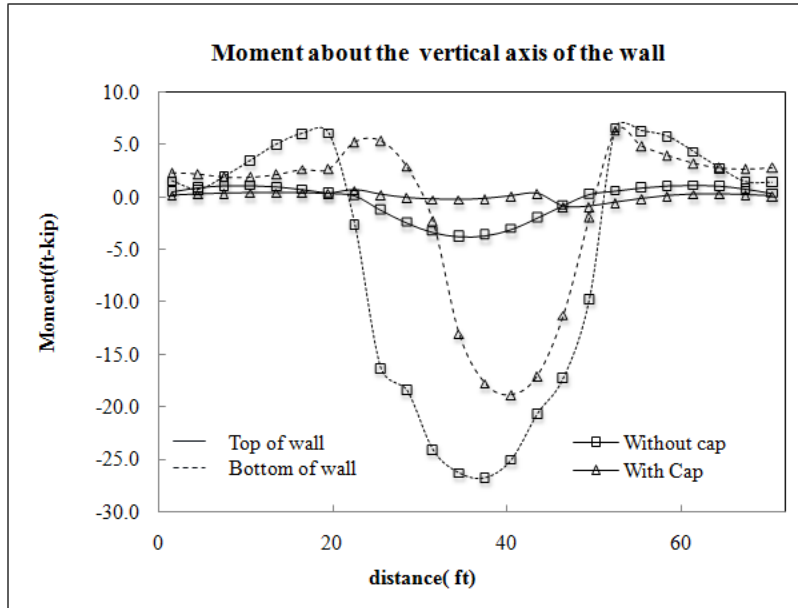


Fig 32: Moment about the vertical axis of the wall

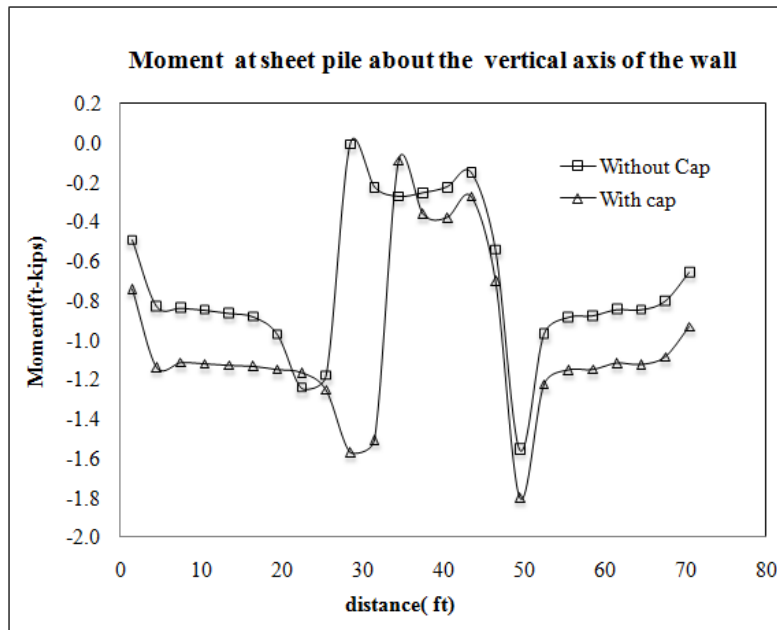


Fig 33: Moment at the sheet pile about the vertical axis of the wall

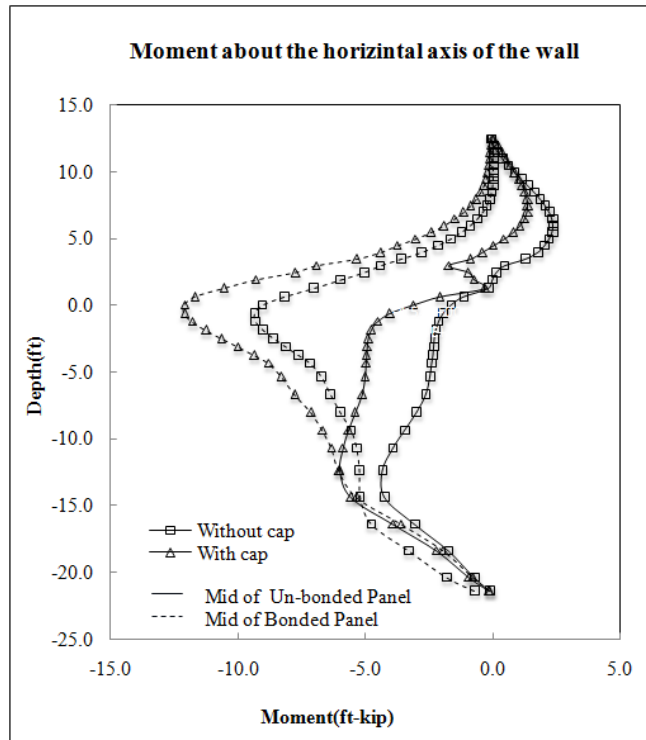


Fig 34: Moment about horizontal axis of the wall

In this case, there has been a significant reduction of both the relative displacement and the overall displacement on the two adjacent panels when cap is installed. Also the moment distribution has been significantly changed due to the installment of the cap. As in the first case, the computed moment and the moment of the resistance of the typical I-wall is compared and is shown in the Table 4:

Table 4: Comparison between the computed bending moment and the moment of resistance

S/N	Section	Moment of resistance (ft-lb)				Computed moment (ft-lb)
		Real strength		ASTM Design Strength		
		Assumpt.1	Assumpt.2	Assumpt.1	Assumpt.2	
1	a	40,416.75	52,629.62	34,155.00	44,045.38	12100
2	b	12,593.63	24,430.92	10,642.50	20,222.76	4380
3	c	28,681.78	39,175.00	24,238.13	32,825.03	26800
4	d	8,872.78	19,366.00	7,498.13	16,085.03	3770

In this case also, maximum moment in the sheet pile computed by FLAC^{3D} is 12100 lb-ft (M_y) and 1570 lb-ft (M_x). For these moments, the stresses developed in the sheet pile due to M_y is 0.39ksi and due to M_x is 0.05 ksi which are far below the yield strength of the sheet pile.

Conclusion

The main objective of this study was to evaluate the performance of the structural cap. But after the comprehensive analysis, the results are not that persuasive to confirm the effectiveness of the cap in reducing the overall displacement of the system. From the study, it was found that the structural cap is effective in restricting the relative displacement of the adjacent panels but is not that effective in reducing the overall displacement of the system significantly in first two cases but it is very effective to reduce the overall displacement of the system in the third case. The moment distribution was also not that improved by the incorporation of the cap. But still we can convince our self to one point that since the relative displacement has been totally restricted, the

cap has somewhat tried to integrate the panels in one system. This would eventually prohibit the localized weak panel to fall individually by supported by the other panel.

The other outcome of this analysis was that the spatial variation of the strength non uniform erosion along the I-wall results the higher bending moment about the vertical axis which is not addressed in the current design guidelines. This can be seen by comparing the moment of resistance of the typical cross section with the computed bending moment. On top of that the typical section of the I-wall even fails to satisfy the minimum reinforcement requirement which is given by the relation (ACI 1984):

$$\rho_{\min} = \frac{200}{f_y}$$

For, f_y 60 ksi, ρ_{\min} is 0.0033, but the for the typical section, ρ calculated is only 0.0029 for the section at top of wall and 0.0012 for the section at the bottom of wall.

As an evidence to support the flaw in design guidelines, Seed et al. (2008) pointed out that most of the concrete capping of the South breach of IHNC was spalled since the concrete couldn't withstand the tensile stress caused by the excessive bending of the I-wall due to erosion. As already discussed, the final breach scenario that was observed during Katrina was only possible due to the progression of the local breaches. The initiation of the breach might have started by the localized spall of the concrete panel due to high bending stress. This spall of the concrete capping would result in the uncontrolled erosion and thus expanding the breach wider and wider in an exponential manner. So if only the initiation of the breach can be restricted, we don't have to worry about the large global breach.

Modeling the full phase breach is not possible numerically. From the numerical simulation we can only observe the onset of the breach and the factors that led to such failures. But it can still be explained that the full breaching of I-wall during hurricane Katrina must be a result of the propagation of the small scale localized failure and this propagation rate must be higher and higher as time passes within the time span between the onset of the localized breach and the final global breach.

We are now in a position to say that the bending stresses developed due to the local breaches and the erosion should be looked upon seriously and should be incorporated in the design guidelines. Some may argue that the bending stresses developed due to this condition are manifold high that construction of such structure will be very uneconomical. But the point is that the bending stress developed for the final breach may be high but it is not that high during the onset of the failure (stresses found from this study). And if we can design the section to withstand the onset of the localized structural failure, we may overcome the problem created by the large breaching.

So from this study, it may be logical to conclude that though we have to include cap for the integrity of the I wall system, the moment induced by the variation of the shear strength and non uniform erosion along the I-wall section should be in the forefront of the factors while designing the I-wall section for the new construction.

Notation

The following symbols are used in this paper

I_{uncr}	=	moment of Inertia for the uncracked RCC section
b	=	width of the section
D	=	Overall depth of the I-wall section
n	=	modular ratio
A_s	=	area of steel in tension zone
A'_s	=	area of steel in compression zone
h_s	=	distance of the centroidal axis of the tension steel bar to the centroidal axis of the section
h'_s	=	distance of the centroidal axis of the compression steel bar to the centroidal axis of the section
I_{cr}	=	moment of Inertia for the cracked RCC section
d	=	effective depth of the section
d'	=	cover at the compression zone
ρ	=	ratio of the area of steel in tension zone to the effective area of the section
ρ'	=	ratio of the area of steel in compression zone to the effective area of the section
E_c	=	concrete elastic modulus
I_c	=	moment of inertia of the concrete section
E_e	=	equivalent modulus of elasticity corresponding to cracked or uncracked RCC section
t_e	=	equivalent thickness of the section corresponding to cracked or uncracked section
f_{ct}	=	tensile strength of concrete
f_c	=	compressive strength of the concrete
M_{cr}	=	cracking moment
I_e	=	effective moment of inertia for the cracking section
M_a	=	maximum moment in the member at the loading stage
M	=	bending moment at any element of the structural element
ϕ	=	factor for resistance
ϕM_n	=	factored resisting moment
M_n	=	resisting moment
ν	=	Poisson's ratio
c_{11}, c_{22}	=	Stiffness in the global system
c_{12}, c_{33}	=	Stiffness in the global system
c'_{11}, c'_{22}	=	Stiffness in the local system
c'_{12}, c'_{33}	=	Stiffness in the local system
c^{b}_{11}, c^{b}_{22}	=	bending Stiffness in the local system

c_{12}^b, c_{33}^b	=	bending Stiffness in the local system
c_{11}^m, c_{22}^m	=	membrane Stiffness in the local system
c_{12}^m, c_{33}^m	=	membrane Stiffness in the local system
M_x	=	Bending moment about the vertical axis of the wall
M_y	=	Bending moment about the lateral axis of the wall
f_y	=	yield strength of steel
C_s	=	Compressive force in steel
C_c	=	compressive force in concrete
a	=	depth of the compression stress block
ϵ'_s	=	strain at the compression steel

References

- American Concrete Institute (ACI). (2005). "Building Code Requirements for Structural Concrete (ACI 318-05) and Commentary (ACI318R-05)", Detroit
- Bowles, J. E. (1996) "Foundation Analysis and design", McGraw-Hill, New York
- Duncan, M., Brandon, T. L., Wright, S.G. and Vroman, N.(2008) "Stability of I-walls in New Orleans during Hurricane Katrina" *J. of Geotech. Geoenviron. Eng.*, 134(5), 681-691
- Everard, N.J. (1993) "Reinforced Concrete Design" *Serviceability and Deflections* McGraw-Hill, New York, 162-178
- Interagency Performance Evaluation Task Force (IPET) (2007) "Performance evaluation of the New Orleans and southwest Louisiana hurricane protection system" *Final Report of the IPET*
- Itasca Consulting Group, (2006) "FLAC3D Manual", Minneapolis, Minnesota
- MacGregor, J.G. (1992) "reinforced Concrete Mechanics and Design" *Serviceability*, Englewood Cliffs: Prentice Hall, 314-348
- MacGregor, J.G. (1992) "reinforced Concrete Mechanics and Design" *Flexure: T Beams, Beams with compression reinforcement, and special cases*, Englewood Cliffs: Prentice Hall, 126-167
- Seed R.B., Bea, R.G., Athanasopoulos-Zekkos, A, Boutwell, G.P., Bray, J.D.; Cheung, C., Cobos-Roa, D., Ehresing, L., Harder, L.F., Pestana, J.M., Riemer, M.F., Rogers, J.D., Storesund, R., Vera-Grunauer,X. and Wartman, J.(2008) " New Orleans and Hurricane Katrina.II: The Central Region and the Lower Ninth Ward" *J. of Geotech. Geoenviron. Eng.*, 134(5), 718-739
- Ugural, A.C.(1981) " Stresses in Plates and Shells" McGraw-Hill, New York,1-16
- U.S. Army Corps of Engineers (1994) "Engineer Manual 1110-2-2504: Design of sheet pile wall" *Geotechnical Investigation*, Washington DC, 3/1-3/11
- U.S. Army Corps of Engineers (2001) "Plans for Lake Pontchartrain, Louisiana and vicinity hurricane protection High level Plans Orleans Parish, LA" *London Avenue outfall Canal, Parallel Protection*, New Orleans, LA
- U.S. Army Corps of Engineers (2006) "Performance evaluation of the New Orleans and Southeastern Louisiana hurricane Protection system" *Rep. of the Interagency performance evaluation Task Force*, Washington, D.C. (<http://IPET.wes.army.mil>)
- U.S. Army Corps of Engineers and St. Louis District Corps of Engineers (2008) "The London Avenue Site Specific Load Test-Appendix D", New Orleans, LA
(http://www.mvn.usace.army.mil/hps2/hps_reports.asp)

Wang, C., Salmon, C.G.(1998) “Reinforced Concrete Design” *Introduction, Materials, and Properties*, Addison-Wesley , Menlo Park, California ,1-31

<http://www.sheetpiles.net/>